Nanotechnology **19** (2008) 095507 (5pp) doi:10.1088/0957-4484/19/9/095507

Desorption kinetics of oxygen in plasma treated SWNTs by *in situ* thermoelectric power measurements

S C Desai[1], K P Hewaparakrama[2], C Jayasinghe[3], D Mast[3], B K Pradhan[4] and G U Sumanasekera[1,2,5]

[1] Department of Electrical and Computer Engineering, University of Louisville, Louisville, KY 40292, USA
[2] Department of Physics, University of Louisville, Louisville, KY 40292, USA
[3] Department of Physics, University of Cincinnati, Cincinnati, OH 45221, USA
[4] Columbian Chemicals Company, Marietta, GA 30062, USA

E-mail: gusuma01@gwise.louisville.edu

Received 18 September 2007, in final form 26 December 2007
Published 11 February 2008
Online at stacks.iop.org/Nano/19/095507

Abstract
The functionalization and defect formation of SWNTs caused by isotropic plasma treatments were studied using oxygen desorption/adsorption kinetics by measuring the time dependence of the *in situ* thermoelectric power (TEP). It is shown that the plasma treatments result in the formation of low binding energy sites for oxygen adsorption. Raman and x-ray photoelectron spectroscopy (XPS) data are in good agreement with the results.

1. Introduction

The unique electrical properties of single walled carbon nanotubes (SWNTs) continue to attract worldwide attention for further study related to sensor properties. A great deal of research has been directed towards better understanding of the fundamental properties of carbon nanotubes in gas adsorption/desorption. Several groups [1, 2] have observed changes in the electrical conductance of SWNTs during gas or chemical adsorption which has increased interest in the study of SWNTs as gas/chemical sensors. This study can help in showing a clear interdependence of molecular adsorption and transport properties. Recent studies [3] have shown that SWNTs are extremely sensitive to the presence of molecular oxygen. Several groups [3–5], have reported changes in electrical resistivity and thermoelectric power (S) of the SWNTs upon exposure to molecular oxygen. They have argued that SWNTs can be easily doped with O_2 under ambient conditions, forming a weak charge transfer complex ($C_p^{+\delta}O_2^{\delta-}$), where adsorbed oxygen changes the sign of the thermopower. This is similar to what has been also observed for multiwalled carbon nanotubes and activated carbon fibers. However, this conclusion has been contested via the study on field effect transistor (FET) properties of SWNTs by Avouris and co-workers [6], who found that O_2 dopes the electrical contacts made to the SWNTs, and not the wall. In a later publication, Ulbricht *et al* [7], argued that the minority oxygen species located either at defect sites on the SWNT bundles or at tube–metal contacts in the electronic devices are responsible for the observed p-type doping. Several mechanisms have been proposed to explain such phenomena. The gas molecules could affect the transport properties indirectly by binding to the donor or acceptor centers in the substrate, at the contacts, or directly by binding to the nanotube surface. In the latter case, the gas could be either physisorbed (bound by dispersive van der Waals forces) or chemisorbed (bound by the formation of a chemical bond resulting in charge transfer between the nanotube and the gas molecule). This adsorption could take place either on the walls of a perfect nanotube or at the defect sites. Experimentally, one way to differentiate physisorption from chemisorption is by checking for a linear relationship between the thermoelectric power and the additional resistance induced by gas adsorption [3]. This method supports the idea of O_2 being chemisorbed on SWNTs. However, a recent experimental study of the kinetics of oxygen adsorption and desorption on SWNTs shows that the estimated binding energy is low and is consistent with physisorption of oxygen in molecular form [7]. But it remains unclear whether atomic or

[5] Author to whom any correspondence should be addressed.

molecular oxygen is responsible for the charge transfer. Recent experiments done by Tchernatinsky *et al* [8], which were based on an individual semiconducting SWNT based FET, showed that the oxygen adsorption is indeed physisorption. Impurity states generated by O_2 pin the Fermi level near the top of the valence band of the nanotube, resulting in the observed p-type behavior of the oxygen rich SWNT. The adsorption/desorption kinetics of oxygen in SWNTs have been explored by various groups [3, 4, 6–9]. Similar to the FET device study, it has been seen that the TEP of an oxygen rich nanotube is positive, and is governed by the oxygen impurity present, and that the TEP of an oxygen deficient nanotube remains negative, and is governed by the intrinsic defects/functionalizations on the surface of the nanotube [7]. While there is still a debate over the real mechanism of the effect of oxygen on the electrical properties of SWNTs, a general consensus has been reached that oxygen is responsible for the observed transport properties regardless of whether the oxygen is located at the contacts or on the SWNTs.

There have been several recent reports on the effect of plasma treatment on the surface of SWNTs [10–14]. During the plasma process, excited electrons, ions, and free radicals are generated via inelastic collisions of energetic electrons and molecules. These plasma species can be highly reactive towards the surfaces of the SWNTs, leading to surface modifications.

Here we present reports on the effect of oxygen and argon plasma on purified SWNT bundles by studying the time-dependent TEP behavior of each of these samples during oxygen adsorption/desorption. Raman spectroscopy and x-ray photoelectron spectroscopy (XPS) were also conducted on these samples to confirm the structural properties of these nanotube bundles.

2. Experimental details

The SWNT material in this study was obtained from Carbolex, Inc., and consisted of SWNTs produced by the arc discharge method. These samples were subjected to a post synthesis process of selective oxidation and HNO_3 refluxing as explained elsewhere [15]. The oxidation process helps in removal of carbonaceous impurities and the acid refluxing helps in removal of catalytic metallic impurities which are used during the synthesis of the SWNTs [15–18]. The samples were then subjected to high temperature annealing process in which they were heated to 1200 °C at a pressure of 10^{-7} Torr for 24 h. The oxygen and argon plasma treatments were done on the annealed samples for the further modification of the surface. The plasma treatment was done using an inductively coupled plasma system [10]. The purified nanotubes were stirred at the bottom of a glass reactor using a magnetic bar. The system pressure was measured by a thermocouple pressure gage. A discharge by an RF signal of 13.56 MHz was used for the plasma generation. Before the plasma treatment, the base pressure was pumped down to less than 30 mTorr before the gases were introduced into the reactor chamber. The operating pressure was adjusted by a mass flow controller. The parameters for the plasma were set to a pressure of 350 mTorr, and a power of 125 W, and the exposure for each plasma was 30 min.

For the electrical transport study, the samples were dispersed in dimethyl formamide (DMF) solvent and then drop dispersed onto a glass substrate. The thermopower measurements were conducted on each sample during degassing the sample at 180 °C in a vacuum of 10^{-7} Torr. Two chromel–alumel thermocouples (all 0.003 inch diameter wires) were attached to the edges of the sample with a small amount of silver epoxy to measure the thermoelectric power (TEP). The thermoelectric power data were collected using a heat pulse technique [18]. The sample was placed in an apparatus equipped with a turbo-molecular pump capable of evacuating to 10^{-7} Torr for *in situ* studies which can be heated to 1200 °C inside a tube furnace. Treated SWNTs were characterized using Raman spectroscopy at 632 nm laser excitation. The resonant Raman spectra were measured in the backscattering geometry using a Renishaw inVia Raman spectrometer equipped with an Olympus microscope to focus the laser beam to a 1 μm diameter spot on the sample. The XPS studies were also performed on these samples using a VG Scientific x-ray photoelectron spectrometer with an XR3E2 x-ray source system.

3. Results

In figure 1, we show the resonant Raman spectra for the pristine, argon plasma treated, and oxygen plasma treated samples, respectively, from bottom to top, taken at 632 nm laser excitation. All the spectra show clear features corresponding to the G band with upper and lower G^+ and G^- components (tangential C–C vibrations), D band (disorder induced), G′ band (second order of the D band associated with a double phonon process) and the RBMs (radial breathing modes) inherent for SWNTs. All D, G′ and RBM bands are seen to upshift with the plasma treatments. This can be attributed to the compression (hardening) of the C–C bonds caused by plasma exposure. Further, the D band to G band ratio seems to increase with the plasma treatment, as shown in the inset of the figure 1. This is a further indication of the infliction of defects on the SWNTs during the plasma treatment.

Figure 2 shows the XPS data for the three samples. Figures 2(a) and (b) show, respectively, the narrow scan XPS spectra for the regions of core levels, C 1s and O 1s, for the annealed, argon plasma treated, and oxygen plasma treated samples, respectively, from bottom to top. A typical curve fitting of the C 1s peak region around ∼284 eV is shown in figure 2(a) for all three samples. It was found that the C 1s peak for all three samples can be fitted very well with three Gaussian line shapes with binding energies at ∼284, 285, and 287 eV. These different binding energy peaks are assigned to C–C (284 eV), C–O (285 eV), and O=C–O (287 eV). The plasma treatments induce defects as well as adding side wall functionalization to the SWNTs. The main peak at 284 eV corresponding to sp^2 hybridized graphitic carbon (C–C bonds) of the C 1s peak is observed to upshift, implying hardening of the C–C bonds (compression) during plasma treatments, consistent with Raman results. The relatively weak band

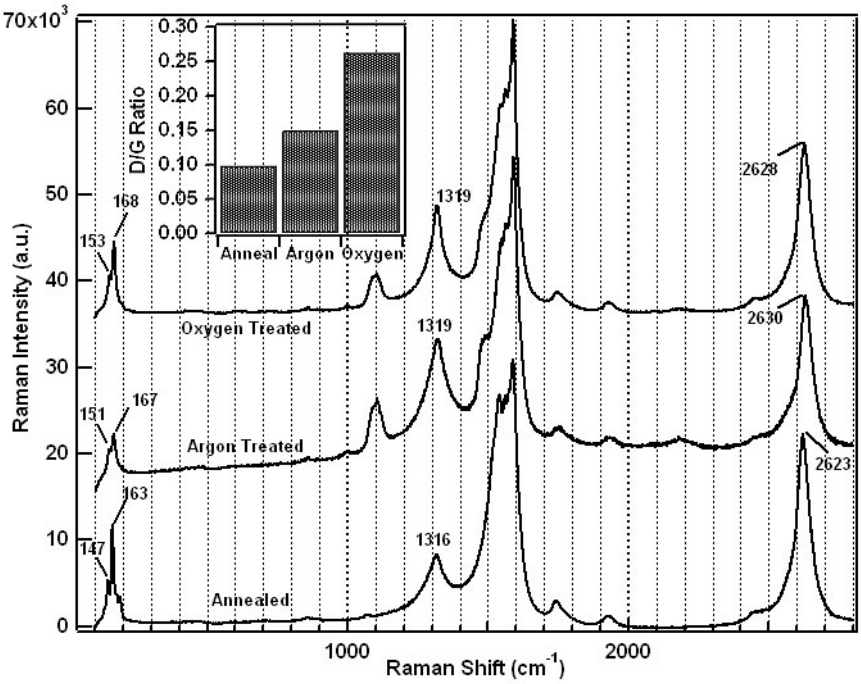

Figure 1. Raman spectra at 632 nm laser excitations for pristine, argon plasma treated, and oxygen plasma treated SWNTs, respectively, from bottom to top. The inset shows the histogram of the D band to G band intensity ratio for the three samples.

corresponding to the O=C–O bond in the argon plasma treated sample is due to the removal of most of such surface oxygen during Ar plasma treatment. The O 1s spectra of the three samples which show a peak at 530 eV do not show noticeable shift in the peak positions due to Ar plasma treatment, implying only weak interaction of oxygen and carbon atoms in the SWNTs. As expected, the oxygen treated sample shows an upshift in the O 1s peak.

The time dependence of the thermopower during desorption of oxygen for the three samples are shown in figure 3(a). The reactor was evacuated using a turbo-molecular pump and the temperature was gradually increased until the onset of desorption was observed by the decrease of the thermopower. In figure 3(a), the region corresponding to the negative times shows the initial change of the thermopower while the required temperature ($\sim$180 °C) is reached. The pristine sample shows negligible drop of thermopower (-0.003 μV min^{-1}) and the argon plasma treated sample shows relatively faster drop in the thermopower (-0.016 μV min^{-1}) in this initial period. Interestingly, the oxygen plasma treated sample shows the fastest drop in thermopower (-0.361 μV min^{-1}). Once the target ($\sim$180 °C) temperature is reached the TEP of all three samples is seen to drop drastically at that constant temperature, as shown in the region corresponding to positive timescale in the figure. The best fit with three exponentials for each curve is shown in the figure 3(a) for the desorption at constant temperature. It was necessary to include at least three exponents to fit the data. These observations show that oxygen has at least three adsorption sites available in SWNT bundles corresponding to the three exponentials. We believe that these adsorption sites correspond to the interstitial channels, the grooves, and the surfaces of the SWNTs. In the annealed (purified) nanotubes, we believe that the tube ends are closed and that the interiors are not accessible for oxygen adsorption. These three sites with different binding energies for oxygen adsorption result in different time constants. The comparison of the desorption graphs for the three samples reveals that desorption of oxygen for the SWNTs treated with oxygen plasma is faster than that of the argon treated sample and the pristine sample at a given temperature. This can be understood as being due to the formation of low binding energy sites for oxygen desorption as a result of plasma treatments. As evidenced from the Raman and XPS results, the formation of compressed (hardened) C–C bonds can lead to weaker C–O or O=C–O bonds. Even the presence of small amount of weaker C–O bonds can lead to easy removal of such surface oxygen and will be reflected in the TEP data. The argon treated sample shows slower desorption kinetics compared to the oxygen treated sample, but faster kinetics compared to the pristine sample. The argon plasma treatment also inflicts low binding energy sites for oxygen but to a lesser extent compared to the oxygen treated sample. Due to the presence of these low binding energy sites, oxygen can desorb relatively easily compared to the pristine sample. So, in the case of the argon plasma treated sample, the oxygen is loosely bound to the walls of the tubes compared to the pristine sample. Hence, the loosely bound oxygen molecules are relatively easy to be desorbed and result in a shorter time for the thermopower to saturate compared to tightly bound oxygen in the pristine sample.

By assuming that the process is a non-equilibrium surface reaction, the surface reaction rate is equal to the adsorption rate

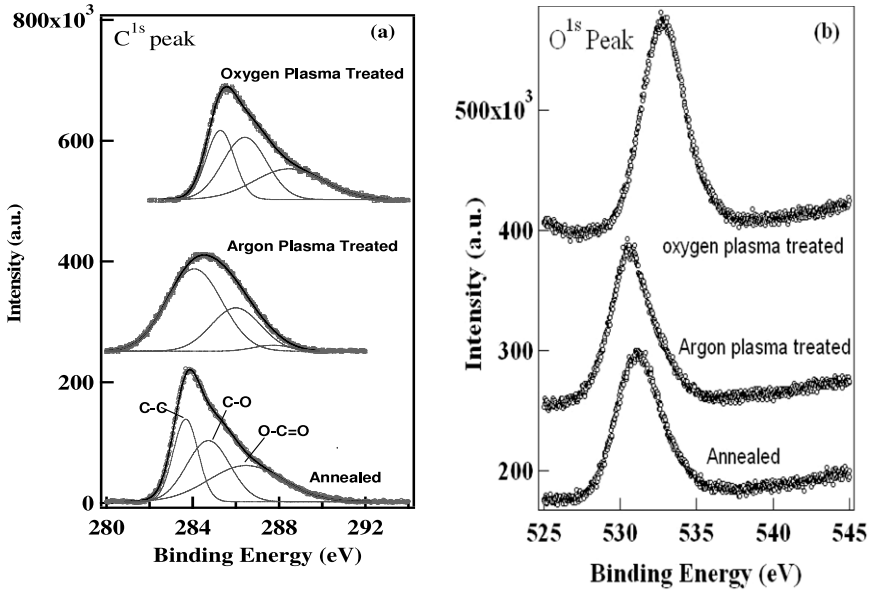

Figure 2. XPS data for annealed, argon plasma treated, and oxygen plasma treated SWNTs, respectively, from bottom to top: (a) C 1s peak with best fits to three Gaussians corresponding to C–C, C–O, and O–C=O bonds; (b) O 1s peak.

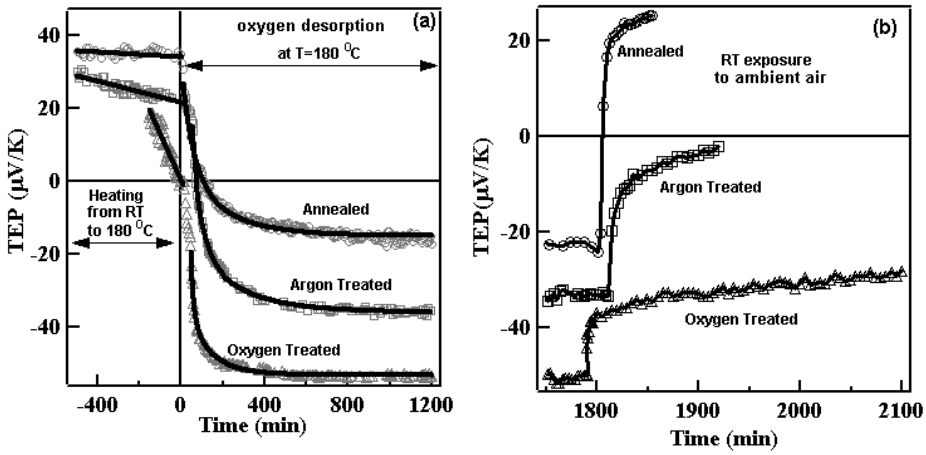

Figure 3. (a) Thermopower versus time for annealed, argon plasma treated, and oxygen plasma treated samples during desorption of oxygen. The region corresponding to the negative times shows the initial change of the thermopower while the required temperature (∼180 °C) is reached. The desorption at this constant temperature is shown in the region corresponding to the positive timescale. Best fits with three exponentials are shown in solid lines. (b) Adsorption kinetics for annealed, argon plasma treated, and oxygen plasma treated samples when exposed to air at room temperature.

minus the desorption rate, i.e.,

$$\frac{\mathrm{d}q}{\mathrm{d}t} = k_{\mathrm{a}}(1-q) - k_{\mathrm{d}}q, \tag{1}$$

where k_{a} is the adsorption rate constant, k_{d} is the desorption rate constant, and q is the number of occupied sites. In figure 3(b), the adsorption kinetics for the three samples is shown when each sample is exposed to ambient air at room temperature. It should be emphasized that the adsorption is a dynamic process with adsorption and desorption taking place simultaneously. The pristine sample recovers its original positive thermopower values rather quickly, within less than 5 min. The argon treated sample requires over an hour to reach a positive thermopower value. Interestingly, the thermopower of the oxygen plasma sample remains negative even after several days. We can understand the adsorption behavior with the help of equation (1). For higher binding energy sites (annealed samples) the adsorption rate constant (k_{a}) is higher, but the slow desorption rate (k_{d}) causes the overall surface reaction to be rather slow. In the presence of low binding energy sites (plasma treated samples), the adsorption rate is slower, but the faster desorption can lead to a faster overall surface reaction.

Figure 4 shows the oxygen desorption results for HiPCO samples subjected to similar plasma treatments (both argon and oxygen). The desorption kinetics are quite similar to previous sample with oxygen plasma treated sample showing faster kinetics followed by argon plasma treated and pristine

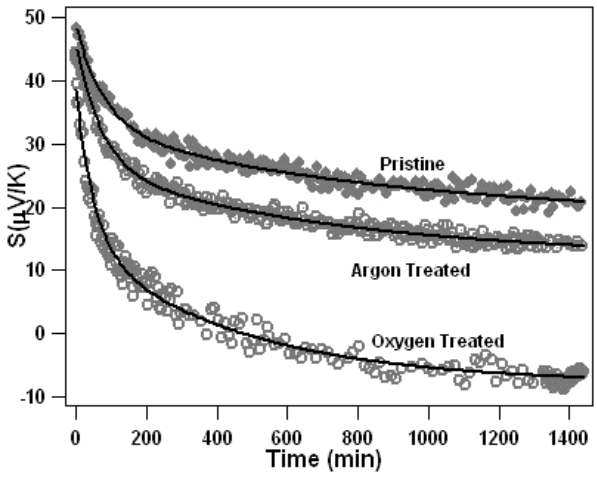

Figure 4. Thermopower versus time for three HiPCO samples during desorption of oxygen. Best fits with three exponentials are also shown in solid lines.

SWNTs respectively. The solid lines are again the best fits with three exponentials.

4. Conclusion

Isotropic plasma treatment with different gases at varying pressure and plasma power provides a way of introducing defects on SWNT walls in a controllable way. Raman and XPS data show that the structural integrity of the SWNTs is still retained after the plasma treatment, but the treatment causes uniaxial constriction, resulting in compressed C–C bonds. In turn these compressed C–C bonds cause a certain amount of weaker carbon–oxygen bonds with lower binding energies. *In situ* thermopower data show faster desorption in the presence of such low binding energy sites. This can have an impact on improving the response time in SWNT based gas sensors.

Acknowledgment

We acknowledge discussions with Professor Shi-Yu Wu on various results on numerous occasions during this project.

References

[1] Kong J, Franklin N R, Zhou C, Chapline M G, Peng S, Cho K and Dai H 2000 *Science* **287** 622
[2] Collins P G, Bradley K, Ishigami M and Zettl A 2000 *Science* **287** 1801
[3] Sumanasekera G U, Adu C K W, Fang S L and Eklund P C 2000 *Phys. Rev. Lett.* **85** 1096
[4] Hone J, Ellwood I, Muno M, Mizel A, Cohen M L and Zettl A 1998 *Phys. Rev. Lett.* **80** 1042
[5] Jhi S H, Louie S G and Cohen M L 2000 *Phys. Rev. Lett.* **85** 1710
[6] Derycke V, Martel R, Appenzeller J and Avouris Ph 2001 *Nano Lett.* **1** 9
[7] Ulbricht H, Moos G and Hertel T 2002 *Phys. Rev.* B **66** 075404
[8] Tchernatinsky A, Desai S, Sumanasekera G U, Jayanthi C S, Nagabhirava B, Alphenaar B W and Wu S Y 2006 *J. Appl. Phys.* **99** 034306
[9] Adu C K W, Sumanasekera G U, Pradhan B K, Romero H E and Eklund P C 2001 *Chem. Phys. Lett.* **337** 31
[10] Utegalav Z N, He P, Shi D, Gilland R F and Mast D 2005 *J. Appl. Phys.* **97** 104324
[11] Valentini L, Lozzi L, Cantalini C, Armentano I, Kenny J M, Ottaviano L and Santucci S 2003 *Thin Solid Films* **436** 95
[12] Shi D and He P 2004 *Rev. Adv. Mater. Sci.* **7** 97
[13] Valentini L, Puglia D, Armentano I and Kenny J M 2005 *Chem. Phys. Lett.* **403** 385
[14] Yan H Y, Zhou Q, Li C M, Yue Y C and Chan-Park M B 2005 *Appl. Phys. Lett.* **87** 213101
[15] Liu J, Dai H, Hafner J H, Huffman C B and Smalley R E 1998 *Science* **228** 1253
[16] Rinzler A G, Liu J, Dai H, Huffman C B, Eklund P C, Rao A M and Smalley R E 1998 *Appl. Phys.* A **67** 29
[17] Harutyunyan A R, Pradhan B K, Chang J, Chen G and Eklund P C 2002 *J. Phys. Chem.* **106** 8671
[18] Sumanasekera G U, Grigorian L and Eklund P C 2000 *Meas. Sci. Technol.* **11** 273